Magnetic Disorder in the Frustrated Antiferromagnet Jarosite Arising from the $H_3O^+\cdots OH^-$ Interaction

Daniel Grohol and Daniel G. Nocera*

Department of Chemistry, 6-335, Massachusetts Institute of Technology, 77 Massachusetts Avenue, Cambridge, Massachusetts 02139-4307

Received November 22, 2006. Revised Manuscript Received March 16, 2007

Iron jarosite solid solutions with varying K^+/H_3O^+ ratios have been prepared and their magnetic properties investigated. The jarosite samples, with formulas $K_x(H_3O)_{1-x}Fe_3(OH)_6(SO_4)_2$, ($0 < x < 1$), have been characterized by means of IR spectroscopy, elemental analysis and SQUID magnetic measurements. The ordering temperatures T_{max} of these spin-frustrated antiferromagnets generally decrease with increasing content of interlayer hydronium ions. Magnetic disorder resulting from an interaction between the interlayer hydronium ions and the intralayer $Fe^{3+}-OH^--Fe^{3+}$ groups appears to be responsible for the decrease in T_{max} values with an increasing hydronium content. The $H_3O^+\cdots OH^-$ interaction appears to exercise a more significant impact on the magnetic disorder in jarosites than the extent occupancy of the magnetic Fe^{3+} ions.

Introduction

The phenomenon of spin-frustration presents an intriguing challenge in contemporary condensed matter science[1−3] partly due to the unpredictability of its spin behavior and the emergence of degenerate ground states with fascinating properties,[4−8] and partly due to its relevance in explaining magnetic phenomena such as high T_C superconductivity[9] and the anomalous Hall effect.[10] Theoretical studies have been carried out and predictions made on 2D spin-frustrated triangular and *kagomé* models.[11−14] However, few real compounds with undistorted, high-symmetry structures exist in which this phenomenon can be observed and studied experimentally. One of the very few kagomé structure types in which spin frustration has been observed experimentally is the jarosite family of materials.[15] These inorganic layered materials[16] with general formula $A^IM^{III}_3(OH)_6(SO_4)_2$ usually contain monovalent A^+ ions (Na^+, K^+, Rb^+, Tl^+, Ag^+, NH_4^+, H_3O^+, etc.)[17,18] and trivalent transition metal ions M^{3+}. The jarosite layers are made up of in-plane corner-sharing $M_3(OH)_6(SO_4)_2^-$ trimers that are composed of $M^{III}O_6$ octahedra capped by SO_4 tetrahedra (Figure 1). The interlayer space is filled with the monovalent ions A^+ ions that set the interlayer distance. Unit cell constant *c* comprises three layers. For hydronium jarosite, $c = 17.019(3)$ Å.[19] Among the pure Na, K, and Rb jarosites, the *c* values are 16.605(10), 17.185(2), and 17.568(3) Å, respectively.[17] Of the three A^+ ions, the size of the potassium ion thus best approximates the size of the hydronium, and of the three available choices, the composite K^+/H_3O^+ jarosite suffers the least from size differences between the different monovalent ions.

The unpaired spins in jarosites are magnetically frustrated when $M = Fe^{3+}$ [17,20−24] or $M = Cr^{3+}$,[25−27] due to antiferro-

(1) Ramirez, A. P. *Annu. Rev. Mater. Sci.* **1994**, *24*, 453−480.
(2) Kawamura, H. *J. Phys. Condens. Matter* **1998**, *10*, 4707−4754.
(3) Greedan, J. E. *J. Mater. Chem.* **2001**, *11*, 37−53.
(4) Grohol, D.; Matan, K.; Cho, J. H.; Lee, S. H.; Lynn, J. W.; Nocera, D. G.; Lee, Y. S. *Nat. Mater.* **2005**, *4*, 323−328.
(5) Matan, K.; Grohol, D.; Nocera, D. G.; Yildirim, T.; Harris, A. B.; Lee, S. H.; Nagler, S. E.; Lee, Y. S. *Phys. Rev. Lett.* **2006**, *96*, 247201/1−4.
(6) Shores, M. P.; Nytko, E. A.; Bartlett, B. M.; Nocera, D. G. *J. Am. Chem. Soc.* **2005**, *127*, 13462−13463.
(7) Helton, J. S.; Matan, K.; Shores, M. P.; Nytko, E. A.; Bartlett, B. M.; Yoshida, Y.; Takano, Y.; Qiu, Y.; Chung, J.-H.; Nocera, D. G.; Lee, Y. S. *Phys. Rev. Lett.* **2006**, submitted for publication, cond-mat/0610539.pdf.
(8) Ofer, O.; Keren, A.; Nytko, E. A. Shores; M. P.; Bartlett, B. M.; Nocera, D. G.; Baines, C.; Amato, A. *Phys. Rev. Lett.* **2006**, submitted for publication, cond-mat/0610540.pdf.
(9) Aharony, A.; Birgeneau, R. J.; Coniglio, A.; Kastner, M. A.; Stanley, H. E. *Phys. Rev. Lett.* **1988**, *60*, 1330−1333.
(10) Taguchi, Y.; Oohara, Y.; Yoshizawa, H.; Nagaosa, N.; Tokura, Y. *Science* **2001**, *291*, 2573−2576.
(11) Wannier, G. H. *Phys. Rev.* **1950**, *79*, 357−364.
(12) Harris, A. B. *Phys. Rev. B* **1992**, *45*, 2899−2919.
(13) Sachdev, S. *Phys. Rev. B* **1992**, *45*, 12377−12396.
(14) Ritchey, I.; Chandra, P.; Coleman, P. *Phys. Rev. B* **1993**, *47*, 15342−15345.
(15) Nocera, D. G; Bartlett, B. M.; Grohol, D.; Papoutsakis, D.; Shores, M. P. *Chem. Eur. J.* **2004**, *10*, 3850−3859.
(16) Jambor, J. L. *Can. Mineral.* **1999**, *37*, 1323−1341.
(17) Grohol, D.; Nocera, D. G.; Papoutsakis, D. *Phys. Rev. B* **2003**, *67*, 064401/1−13.
(18) Bartlett, B. M.; Nocera, D. G. *J. Am. Chem. Soc.* **2005**, *12*, 8985−8993.
(19) Majzlan, J.; Stevens, R.; Boerio-Goates, J.; Woodfield, B. F.; Navrotsky, A.; Burns, P. C.; Crawford, M. K.; Amos, T. G. *Phys. Chem. Miner.* **2004**, *31*, 518−531.
(20) Takano, M.; Shinjo, T.; Kiyama, M.; Takada, T. *J. Phys. Soc. Jpn.* **1968**, *25*, 902.
(21) Takano, M.; Shinjo, T.; Takada, T. *J. Phys. Soc. Jpn.* **1971**, *30*, 1049−1053.
(22) Townsend, M. G.; Longworth, G.; Roudaut, E. *Phys. Rev. B* **1986**, *33*, 4919−4926.
(23) Wills, A. S.; Harrison, A. *J. Chem. Soc., Faraday Trans.* **1996**, *92*, 2161−2166.
(24) Inami, T.; Maegawa, S.; Takano, M. *J. Magn. Magn. Mater.* **1998**, *177−181*, 752−753.
(25) Keren, A.; Kojima, K.; Le, L. P.; Luke, G. M.; Wu, W. D.; Uemura, Y. J. *Phys. Rev. B* **1996**, *53*, 6451−6454.
(26) Lee, S.-H.; Broholm, C.; Collins, M. F.; Heller, L.; Ramirez, A. P.; Kloc, C.; Buchner, E.; Erwin, R. W.; Lacevic, N. *Phys. Rev. B* **1997**, *56*, 8091−8097.
(27) Inami, T.; Morimoto, T.; Nishiyama, M.; Maegawa, S.; Oka, Y.; Okumura, H. *Phys. Rev. B* **2001**, *64*, 054421/1−6.

10.1021/cm062793f CCC: $37.00
Published on Web 05/15/2007

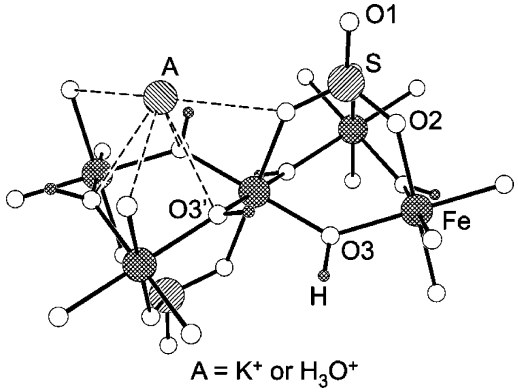

Figure 1. Structure of the magnetic subunit of jarosite.

magnetic nearest neighbor interactions between the M^{3+} ions. In $M = V^{3+}$, these isostructural jarosite relatives show no magnetic frustration due to ferromagnetic nearest neighbor interactions between the V^{3+} ions.[28−31]

Magnetic properties of jarosites are highly sensitive to the purity of samples. Until recently,[17,29] pure and highly crystalline jarosites have been difficult to prepare due to a lack of suitable synthetic method, which made the magnetic characterization of jarosites strongly sample-dependent. It is intuitively apparent that the occupancy disorder of the strongly spin-correlated trivalent centers M^{3+} will introduce deviations from the magnetic behavior of an ideal system with a complete coverage of magnetic sites. Thus, the role of disorder of the magnetic sites M^{3+} in frustrated kagomé lattices has received a significant amount of attention.[32−35] The *nature* of the interlayer cation A^+ can also significantly affect the bulk magnetic properties, particularly if the A^+ ion is reactive with the host kagomé lattice. Until recently, the H_3O^+ ion was thought of in the same way as any other *inert* ion, and a potential impact on the magnetic properties of a $H_3O^+\cdots OH^-$ interaction inside the jarosite lattice was mostly neglected. However, recent studies suggested that alkali jarosites contaminated by H_3O^+ exhibited magnetic disorder owing to the $H_3O^+\cdots OH^-$ interaction in the vanadium jarosite series,[29] and in the iron jarosite series.[17] A subsequent ^1H NMR study[36] supported these findings. In the present study, a series of solid hydronium:potassium jarosite compounds have been synthesized. The long-range order (LRO) of jarosite exhibits a systematic dependence on the H_3O^+ ion concentration; the ordering temperature decreases monotonically with increasing H_3O^+ substitution. The results strongly support the contention that hydronium ions introduce a significant magnetic disorder into the kagomé jarosite framework, thus making the hydronium jarosite a chemically more complicated system than previously believed.

Experimental Section

General Procedures. All chemicals of reagent or analytical grade were obtained from commercial companies, and they were used without purification. Hydrothermal reactions were carried out in 125-mL Teflon-lined pressure vessels, which had been purchased from Parr Instruments. A Fisher Isotemp programmable oven with forced-air circulation was used to obtain the desired temperature profiles for hydrothermal reactions.

Synthesis of Jarosites by Single-Step, Nonredox Methods: Preparation of $K_x(H_3O)_{1-x}Fe_{3-y}(H_2O)_{3y}(OH)_{6-3y}(SO_4)_2$. Hydronium jarosite and the four solid solutions with varying K^+/H^+ ratios were prepared under similar conditions: Into each of five beakers with 50 mL of distilled water, 8.00 g of $Fe_2(SO_4)_3\cdot xH_2O$ ($x \sim 5$) (16.3 mmol) was dissolved. Appropriate amounts of K_2SO_4 were then added: 0, 28.4, 86.0, 114, and 568 mg (0, 0.163, 0.494, 0.652, and 3.26 mmol, respectively). The resulting solutions were filtered and transferred into Teflon liners of 125 mL pressure vessels. The vessels were enclosed and placed into an oven at 150 °C for 8 h. The vessels were then cooled at 0.5 °C min^{-1} to room temperature. Ochre-color suspensions were filtered, extensively washed with distilled water, and dried in air. The pH values of the filtrates ranged between 1.1 and 1.3. The pure, stoichiometric jarosite $KFe_3(OH)_6(SO_4)_2$ was prepared as described earlier.[17] Anal. Calcd for $H_9Fe_3S_2O_{15}$: H, 1.89; Fe, 34.85; S, 13.34. Found: H, 1.70; Fe, 35.65; S, 13.93. Anal. Calcd for $H_{8.55}K_{0.15}Fe_3S_2O_{14.85}$: H, 1.78; K, 1.21; Fe, 34.64; S, 13.26. Found: H, 1.71; K, 1.15; Fe, 35.65; S, 13.96. Anal. Calcd for $H_{8.05}K_{0.31}Fe_3S_2O_{14.68}$: H, 1.67; K, 2.49; Fe, 34.42; S, 13.17. Found: H, 1.59; K, 2.49; Fe, 35.58; S, 12.42. Anal. Calcd for $H_{8.28}K_{0.44}Fe_{2.82}S_2O_{14.59}$: H, 1.74; K, 3.58; Fe, 32.77; S, 13.34. Found: H, 1.58; K, 3.23; Fe, 31.96; S, 14.57. Anal. Calcd for $H_{7.20}K_{0.73}Fe_{2.87}S_2O_{14.27}$: H, 1.48; K, 5.84; Fe, 32.81; S, 13.13. Found: H, 1.40; K, 5.69; Fe, 32.68; S, 12.03. Anal. Calcd for $H_6KFe_3S_2O_{14}$: H, 1.21; K, 7.81; Fe, 33.46; S, 12.81. Found: H, 1.29; K, 7.68; Fe, 33.41; S, 12.94.

Methods. Infrared spectra of jarosites in KBr pellets were recorded on a Nicolet Magna-IR 860 Spectrometer equipped with a KBr beam splitter and a DTGS detector. For each spectrum, 32 scans were acquired with 4 cm^{-1} resolution over a wavelength range of 4000−400 cm^{-1}.

Magnetic susceptibilities of powdered samples were measured in gelatin capsules using a SQUID magnetometer (Quantum Design MPMSR2) over a 6−400 K temperature range at 50 Oe. Curie−Weiss constants were calculated from linear fits of the inverse susceptibilities vs temperature in the range $T = 200-400$ K.

Results

Synthesis. In homogeneous solutions, alkali jarosites precipitate according to the following equation:[37]

$$3Fe^{3+} + 2A_2SO_4 + 6H_2O \rightarrow AFe_3(OH)_6(SO_4)_2 + 3A^+ + 6H^+ \quad (1)$$

If alkali ions are not available in an acidic solution, or are depleted in an acidic solution as a consequence of the above reaction, a hydronium ion H_3O^+ can substitute for the alkali, and the resulting product will have general composition:

(28) Grohol, D.; Papoutsakis, D.; Nocera, D. G. *Angew. Chem., Int. Ed.* **2001**, *40*, 1519−1521.
(29) Grohol, D.; Nocera, D. G. *J. Am. Chem. Soc.* **2002**, *124*, 2640−2646.
(30) Papoutsakis, D.; Grohol, D.; Nocera, D. G. *J. Am. Chem. Soc.* **2002**, *124*, 2647−2656.
(31) Grohol, D.; Huang, Q. Z.; Toby, B. H.; Lynn, J. W.; Lee, Y. S.; Nocera, D. G. *Phys. Rev. B* **2003**, *68*, 094404/1−7.
(32) Earle, S. A.; Ramirez, A. P.; Cava, R. J. *Physica B* **1999**, *262*, 199−204.
(33) Wills, A. S.; Harrison, A.; Ritter, C.; Smith, R. I. *Phys. Rev. B* **2000**, *61*, 6156−6169.
(34) Frunzke, J.; Hansen, T.; Harrison, A.; Lord, J. S.; Oakley, G. S.; Visser, D.; Wills, A. S. *J. Mater. Chem.* **2001**, *11*, 179−185.
(35) Pettigrew, K. G.; Visser, D.; Harrison, A.; Nicholson, D. H.; Kilcoyne, S. H.; Manuel, P.; Murani, A. P. *Can. J. Phys.* **2001**, *79*, 1517−1523.
(36) Nishiyama, M.; Maegawa, S. *Physica B* **2003**, *329−333*, 1065−1066.
(37) Dutrizac, J. E. *Metallurg. Trans. B* **1983**, *14*, 531−539.

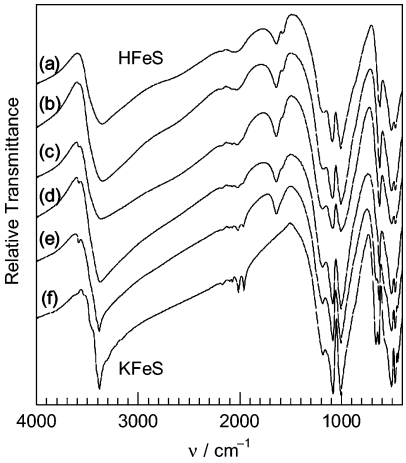

Figure 2. IR spectra of K^+- and H_3O^+-containing jarosites: (a) HFeS, (b) $K_{0.15}$FeS, (c) $K_{0.32}$FeS, (d) $K_{0.44}$FeS, (e) $K_{0.73}$FeS, and (f) KFeS.

$A_x(H_3O)_{1-x}Fe_3(OH)_6(SO_4)_2$, where $(0 < x < 1)$. During this reaction, incomplete hydrolysis often leads to substitution of the H_2O molecules for the bridging OH^- anion, which leads to a local excess positive charge. Every three such disorders are able to displace one Fe^{3+} ion, leading to iron deficiency and to general formula: $A_x(H_3O)_{1-x}Fe_{3-y}(H_2O)_{3y}(OH)_{6-3y}(SO_4)_2$, where $y = 0$. The A^+/H_3O^+ ratio in the jarosite product is affected by the relative concentrations of the respective solubilized ions in the reaction solution. Varying the concentrations of either of these ions in the reaction solution in principle can achieve the same effect, but varying the hydronium content is not practical. Precipitation of jarosite is very pH-dependent: for pH < 0.5, jarosite dissolves, and if pH > 2.5, the product will be contaminated by varying amounts of Fe_2O_3 impurity.

Varying the concentration of the potassium ions in the reaction mixture is thus a better way of controlling the alkali/hydronium ratio in jarosites. A reasonable spread of the x values in $K_x(H_3O)_{1-x}Fe_{3-y}(H_2O)_{3y}(OH)_{6-3y}(SO_4)_2$ has been achieved by keeping the amounts of all other reactants constant, while controlling the concentration of K_2SO_4. The K/Fe molar ratios in the reactant solutions of 0, 0.01, 0.03, 0.04, and 0.2 yielded x values of 0, 0.15, 0.32, 0.44, and 0.73, respectively (abbreviated HFeS, $K_{0.15}$FeS, $K_{0.32}$FeS, $K_{0.32}$FeS, and $K_{0.73}$FeS and for $x = 1$, KFeS).

Single-step precipitation reactions, however, do not provide for very good control of the Fe occupancy, i.e., the y value. In an ideal jarosite lattice, Fe occupancy equals 3, and $y = 0$, but vacancies in the Fe sites represent an inherent drawback of the single-step synthetic route. The end members of the series, HFeS and KFeS, tend to show higher Fe occupancies than the "middle" members. This tendency likely stems in large part from the overall disorder tendencies in mixed-ion samples: the greater the disorder of the A^+ ion, the greater the disorder in the Fe occupancy.[15] Additionally, the local charge imbalance created by the Fe vacancy is stabilized by hydronium ions reacting with unstable terminal Fe−O−H groups to form stable terminal $Fe-OH_2$ groups, as it has been demonstrated in alunite.[38]

Infrared Spectroscopy. IR spectra of all the jarosite samples are shown in Figure 2. The 3500−3000 cm^{-1} region contains an O−H stretching mode. In all jarosites except the pure KFeS, an H−O−H bending mode shows around 1640 cm^{-1}.[39,40] In the spectrum of KFeS, a peak consistent with the Fe−O−H bending overtone shows as a doublet at 2013 cm^{-1}, and this feature broadens as the H_3O^+ content increases. The cluster of several strong peaks centered around 1000 cm^{-1} consists of two antisymmetric S−O stretches of the sulfate group at 1175 and 1085 cm^{-1} and of the Fe−O−H deformation mode 1005 cm^{-1}. Another cluster of peaks found at a still lower energy consists of bending deformations of the SO_4^{2-} ion at 660 and 635 cm^{-1} and of the Fe−O stretching modes at 509 and 472 cm^{-1}.

As the K^+/H_3O^+ ratio varies, several changes can be observed in the spectra. The O−H stretching peak in the pure KFeS derivative is sharp, and it becomes broader as H_3O^+ ions increasingly replace K^+. In KFeS, the O−H stretch arises from the intralayer OH bridging moiety, which gives the peak its sharpness. In jarosites containing some amount of H_3O^+, the O−H stretching peak consists of various contributions from the H_3O^+ ions, as well as from H_2O species created by interactions between the interlayer H_3O^+ ions and bridging OH^- groups. As the amount of H_3O^+ ions increases, the OH contributions from various OH^- environments increase, resulting in the broadening of the O−H stretching peak.

The H−O−H bending mode around 1640 cm^{-1} is absent in pure KFeS, but it is present in all the other derivatives. Note that the intensity of this peak does not increase proportionally to the degree of protonation. The size of this peak for $K_{0.73}$FeS is about the same as that of the pure HFeS. A small shoulder at ∼1580 cm^{-1} is visible in the HFeS spectrum, and it diminishes as $x \rightarrow 1$. In KFeS, the Fe−O−H deformation overtone peaks around 2000 cm^{-1} is sharp and well-resolved. As hydronium replaces potassium, the peaks broaden, and in HFeS, they eventually merge into one very weak and broad band. Similarly, as in the case of the O−H stretch, the broadening is apparently due to a multitude of neighboring interfering O−H oscillators in the Fe−O−H environment. In spite of having been observed in several studies of jarosite compounds,[41−43] this overtone feature was often overlooked and has been assigned in jarosite only relatively recently.[17] It is interesting to note that the definition and shape of this overtone doublet-resembling feature is much more strongly affected by the protonation extent than the width of the strong Fe−O−H parent mode at 1005 cm^{-1}.

Magnetism. Magnetic properties of the jarosite end members HFeS and KFeS, of four solid solutions with gradually changing compositions, and of a physical 1:1 mixture of the end members, were examined by SQUID measurements in the 6−400 K range. Zero-field-cooled (ZFC) and field-cooled (FC) susceptibility measurements

(38) Nielsen, U. G.; Majzlan, J.; Phillips, B.; Ziliox, M.; Grey, C. P. *Am. Mineral*, accepted.
(39) Powers, D. A.; Rossman, G. R.; Schugar, H. J.; Gray, H. B. *J. Solid State Chem.* **1975**, *13*, 1−13.
(40) Nakamoto, K. *Infrared and Raman Spectra of Inorganic and Coordination Compounds*; Wiley: New York, 1986.
(41) Wilkins, R. W. T.; Mateen, A.; West, G. W. *Am. Mineral.* **1974**, *59*, 811−819.
(42) Sasaki, K.; Tanaike, O.; Konno, H. *Can. Mineral.* **1998**, *36*, 1225−1235.
(43) Sasaki, K.; Konno, H. *Can. Mineral.* **2000**, *38*, 45−56.

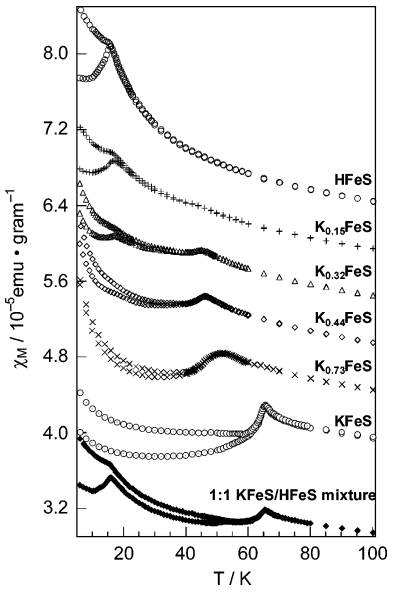

Figure 3. Magnetic susceptibility of K^+- and H_3O^+-containing jarosites.

Table 1. Magnetic Data of K^+- and H_3O^+-Containing Jarosites

compound	Θ_{CW} (K)	T_{max} (K)	T_{max2} (K)	T_D (K)
HFeS	−880	15.7		16
$K_{0.15}$FeS	−860	17.0	44.0	∼40
$K_{0.32}$FeS	−850	17.2	45.0	∼40
$K_{0.44}$FeS	−840		46.2	∼40
$K_{0.73}$FeS	−790		52.0	46
KFeS	−828		65.4	53
KFeS:HFeS (1:1)		15.7	65.4	53

between 6 and 100 K only are shown in Figure 3 and the relevant magnetic data in Table 1.

In low-temperature regions, where ZFC and FC traces diverge ($T < T_D$), the ZFC traces of all measurements are found lower than their FC counterparts. The shapes of the curves, the location of maxima T_{max}, and even the number of maxima vary from sample to sample. The ZFC trace of HFeS (Figure 3) ascends from 6 K to a maximum ordering temperature $T_{max} = 15.7$ K and descends upon further temperature increase. The FC trace for the same compound descends to T_{max}, where it merges with the ZFC curve, and from this point, the traces descend identically. When 15% of the H_3O^+ ions are substituted by K^+ ions to yield $K_{0.15}$FeS, the ZFC maximum shifts to $T_{max} = 17.0$ K. The two traces ZFC and FC do not merge at this T_{max} maximum, but rather at a higher temperature $T_D \sim 40$ K. Above T_{max}, however, the ZFC − FC difference is very small and merging very gradual. A very weak shoulder of a new transition T_{max2} is observed in both the merged traces at ∼44 K.

Increasing the K^+ content further to yield $K_{0.32}$FeS causes the T_{max} peak in the ZFC trace to diminish, and it nearly disappears in the FC trace. Both the ZFC and FC traces very gradually approach each other, until they merge around $T_D \sim 40$ K, with an onset of the second maximum $T_{max2} = 45.0$ K. In the susceptibility of the next representative $K_{0.44}$FeS, the T_{max} maximum practically disappears, leaving but a small shoulder in the ZFC trace at ∼20 K. The ZFC and FC curves merge at $T_D \sim 40$ K, and the T_{max2} maximum increases as it slightly moves to 46.2 K. In $K_{0.73}$FeS, the T_{max} peak has completely disappeared, the ZFC and FC traces merge at $T_D = 46$ K, and the T_{max2} maximum moves up to 52.0 K. For a pure KFeS, $T_D = 53$ K, and $T_{max2} = 65.4$ K, as has been observed previously.[17] The susceptibility data of a 1:1 physical mixture of the end members HFeS and KFeS essentially represent a superposition of the traces of the parent compounds. The T_{max} and T_{max2} maxima occur in the same positions as those of the end members: $T_{max} = 15.7$ K, $T_{max2} = 65.4$ K, and $T_D = 53.0$ K.

Curie−Weiss plots are linear above 150 K for all derivatives, and their extrapolations yield Curie−Weiss temperatures Θ_{CW} between −790 and −880 K (Table 1). These values reflect strong nearest neighbor antiferromagnetic interactions that have been described earlier.[17]

Discussion

The pure potassium jarosite KFeS shows the highest Néel temperature of the series of jarosite solid solutions with variable K^+/H_3O^+ ratios (Figure 3, Table 1). Conversely, the hydronium analogue HFeS shows the lowest T_{max} value of 16 K with the T_{max} values of the other jarosite members with K^+/H_3O^+ ratios falling between the two end members. In addition to the very low T_{max} value, the HFeS jarosite differs from the other Fe jarosites by the absence of magnetic ordering.[23] Thus, a natural question arises of how the H_3O^+ ion fundamentally differs from Na^+, K^+, Rb^+, and NH_4^+ in terms of its impact on the magnetic properties of jarosite? And more generally, how does the nature of the A^+ interlayer ion affect the magnetic ordering?

The nature of the interlayer cation appears to be the only physical factor that, in a significant way, sets the H_3O^+ jarosite radically apart from its alkali and ammonium analogues. This issue has previously been identified,[44] but the implications of the answers for magnetism have mostly been neglected. Three types of A^+ ions have been incorporated into jarosite-type structures. The first group, inert spherical cations A^+ (Na^+, K^+, Rb^+, Tl^+, etc.), do not react *chemically* with their environment within the jarosite lattice; they serve simply as interlayer spacers. Tetrahedral cations such as NH_4^+ ion have more chemical functionality as they can hydrogen bond to oxygen atoms composing the magnetic layers. However, the pK_a's are such that the NH_4^+ ion is chemically rather inert with respect to the jarosite lattice, namely, with respect to its most reactive species, the OH^- group:

$$NH_3 + H_2O \rightleftharpoons NH_4^+ + OH^- \qquad K_b \sim 1.8 \times 10^{-5}\ \text{(aq. solution, 298 K)} \quad (2)$$

$$NH_4^+ \rightleftharpoons NH_3 + H^+ \qquad K_a \sim 5.6 \times 10^{-10}\ \text{(aq. solution, 298 K)} \quad (3)$$

Consistent with this contention, the fundamental magnetic properties of the NH_4−Fe jarosite[17] and of the NH_4−V jarosite[30] do not deviate significantly from their respective alkali counterparts.

Unlike the other two groups of interlayer cations, alkali and the ammonium ions, the hydronium ion will act as more than a mere spectator ion between the jarosite layers. The

(44) Ripmeester, J. A.; Ratcliffe, C. I.; Dutrizac, J. E.; Jambor, J. L. *Can. Mineral.* **1986**, *24*, 435−447.

reaction between hydronium and hydroxide anions is strongly exothermic, and therefore very favorable:

$$H_3O^+ + OH^- \text{ (aq)} \rightleftharpoons 2H_2O \text{ (aq)}\ K_W \sim 10^{14},\quad \Delta H = -55.8 \text{ kJ/mol} \quad (4)$$

In the jarosite lattice, the distance between the hydronium (O4) and the hydroxide (O3) oxygen atoms is rather short, ~2.8 Å (Figure 1). The reactivity between these species will be mitigated to some extent; each bridging OH^- group is stabilized by two adjacent Fe^{3+} ions, and the H_3O^+ group is stabilized by six surrounding sulfate and six hydroxy oxygen atoms. Structural determinations carried out to date on hydronium jarosite indicate significant disorder of the H_3O^+ group. A neutron diffraction structural study indicated the O4 atom was located "above" the unit cell's origin, and it could not pinpoint the precise location of the hydrogen atoms without constraining the hydronium ion.[23] A more recent single-crystal X-ray and synchrotron study could not pinpoint the hydrogen atoms either, but located the O4 atom in the unit cell's origin (0 0 0).[19]

The proximity of a pair of highly reactive species as the H_3O^+ and OH^- ions makes it unlikely that the $H_3O^+\cdots OH^-$ interaction would end at a mere hydrogen bonding. Indeed, small amounts of H_2O molecules have been detected in NMR studies,[38,44] and a strong possibility therefore exists that dynamic proton-transfer takes place:

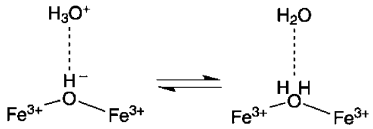

(5)

This type of proton transfer has been found by NMR measurements to be taking place near Al^{3+} vacancies in alunite[38] and has also been observed in jarosite.[45] This type of neutralization accounts for the presence of "excess water," very commonly found in nonstoichiometric jarosites and in alunites.[44,46] Since superexchange between the neighboring metal ions via the p orbitals is the primary mechanism of magnetic exchange in jarosite, proton transfer is expected to affect the magnetic properties—both the nearest neighbor magnetic coupling between the neighboring Fe centers and long-range ordering.

The nature and the magnitudes of the nearest neighbor Fe···Fe magnetic interactions are reflected in Curie−Weiss temperatures, Θ_{CW}. The Θ_{CW}'s of the K_xFeS solid solutions (Table 1) fall within the range of −790 to −880 K. The modest variations in nearest neighbor coupling may be understood when considered in the context of nearest neighbor exchange in isolated binuclear species. In iron-containing[47] as well as vanadium-containing species,[48] protonation of the bridging μ-oxo moiety affects the magnetic exchange rather significantly. In some cases, as for a vanadium biscarboxylate dimer, protonation of the bridging oxo-atom may even turn an antiferromagnetic $V^{III}-O-V^{III}$ interaction into a ferromagnetic one.[49] In binuclear iron complexes, the antiferromagnetic coupling between the centers generally weakens upon protonation of the oxygen-based bridge. The strength of the AF interaction decreases with each protonation step in the order oxo > hydroxo > aquo. This tendency has been demonstrated both experimentally in an acetato-, oxo-bridged complex[47] as well as by the density functional theory (DFT) calculations on a binuclear chloride complex $Cl_3FeOH_xFeCl_3$ ($x = 0, 1, 2$) for a range of Fe−O−Fe angles between 132.5° and 153°.[50] The weakening of the AF coupling parallels a lengthening of the M−O bond upon each protonation step. The 7-fold reduction in AF coupling of the iron dimer is accompanied by a 0.17 Å increase in the Fe−O bond length. In the DFT calculations of the $Cl_3FeOH_xFeCl_3$ complex, the Fe−O bond length increases by 0.15 Å upon protonation from $x = 0$ to $x = 1$, causing a decrease of the AF coupling constant of about 4-fold. Upon the addition of another proton to form an aquo bridge, the Fe−O bond length increases by another 0.33 Å, and the coupling constant weakens another 4-fold. It is clear from these experimental and computational results that the metal−oxygen bond length is a significant determinant of the AF coupling between neighboring Fe centers bridged by oxygen. Against this backdrop, the change in the T_{max} of the K^+/H^+ jarosite samples is noteworthy. The Fe−O3 bond length in pure $KFe_3(OH)_6(SO_4)_2$ is 1.987(2) Å[17] whereas the Fe−O3 bond length in $H_3OFe_3(OH)_6(SO_4)_2$ is 1.9921(8) Å.[23] The difference in the length of the Fe−O3 bond in jarosite is thus only about 0.005 Å. Because such a protonation does not result in the lengthening of the Fe−O3 bond, the nearest neighbor interactions in jarosites are not significantly affected by protonation of the bridging oxygen atom, thus accounting for the narrow range of the Curie−Weiss temperatures across the K^+/H^+ jarosite series (Table 1).

In contrast to nearest neighbor exchange, long-range ordering is affected by the $H_3O^+\cdots OH^-$ interaction quite significantly. Pure potassium jarosite shows magnetic ordering below ~65 K whereas pure hydronium jarosite shows no magnetic order down to 1.5 K.[23] Jarosites of mixed K^+/H_3O^+ concentration exhibit a monotonic decrease in T_{max} with increasing H_3O^+ ion concentration (Figure 3). Proton transfer according to eq 5 is expected to yield varying Js for nearest neighbor interaction, but it does not. A possible explanation is that this dynamic transfer takes place only on relatively few sites at any given time. Since the H^+ transfer is a disordering chemical event in the jarosite lattice, a proton transfer even on very few sites at a time will result in a magnetic disordered state in the whole sample. In this context, it must be noted that proton transfer near Fe^{3+} vacancies that results in total neutralization and in the formation of stable terminal water molecules does not seem to destroy LRO; this was shown in Fe-deficient alkali jarosites.[25] An introduction of a Fe vacancy, and a simultaneous formation of a terminal $Fe-OH_2$ moiety, interrupts the superexchange pathway, which leads to a decrease in the degree of spin ordering which is demonstrated by the

(45) Majzlan, J. Private communication.
(46) Stoffregen, R. E.; Alpers, A. N. *Am. Mineral.* **1992**, *77*, 1092−1098.
(47) Armstrong, W. H.; Lippard, S. J. *J. Am. Chem. Soc.* **1984**, *106*, 4632−4633.
(48) Kanamori, K. *Coord. Chem. Rev.* **2003**, *237*, 147−161.
(49) Knopp, P.; Wieghardt, K. *Inorg. Chem.* **1991**, *30*, 4061−4066.
(50) Chen, Z.; Xu, Z.; Zhang, L.; Yan, F.; Lin, Z. *J. Phys. Chem. A* **2001**, *105*, 9710−9716.

lowering of T_{max}. On the other hand, dynamic proton transfer in pure hydronium jarosite, which likely involves a "proton shuttle" type of disorder, may be the most likely responsible for the fact that hydronium jarosite is the only jarosite with no LRO. This dynamic proton transfer results in the production of relatively few water molecules.

Several of the prepared jarosites show two T_{max} maxima, which also have been observed in previous studies.[24,51,52] Jarosites exhibiting such multiple maxima have always been observed for samples produced from the single-step synthesis route (eq 1). We suspect that this observation is derived in the presence of K^+-rich islands (high T_{max}), and H_3O^+-rich islands (low T_{max}) in the jarosite sample. For a reaction proceeding according to eq 1, the initial reaction solution is relatively K^+-rich and H_3O^+-poor. Since the jarosite lattice prefers the K^+ ions over the H_3O^+ ions, K^+-rich jarosite is expected to form early in the course of the reaction. As jarosite precipitates out, the K^+ ions are gradually depleted, and simultaneously, the H_3O^+ ions are produced. Note that for every 1 mol of jarosite formed, 6 mol of protons are released into the solution. This leads to an increasing proportion of the H_3O^+ ions, which may be incorporated into the jarosite lattice to form H_3O^+-rich jarosite islands. Therefore, the jarosite precipitated at a later stage of the reaction will contain more hydronium ions than jarosite precipitated in the early stage.

In general, such a contamination of alkali jarosites by hydronium ions is difficult to avoid if jarosite is prepared using the single-step synthetic method owing to the proton buildup in the solution. New hydrothermal methods have been developed that circumvent these problems and allow pure jarosite to be prepared by the following sequence of reactions:[17]

$$Fe + 2H_3O^+ \rightarrow Fe^{2+} + H_2 + 2H_2O \quad (6)$$

$$2Fe^{2+} + {}^1/_2O_2 + 2H_3O^+ \rightarrow 2Fe^{3+} + 3H_2O \quad (7)$$

$$3Fe^{3+} + 2A_2SO_4 + 12H_2O \rightarrow AFe_3(OH)_6(SO_4)_2 + 3A^+ + 6H_3O^+ \quad (8)$$

to give an overall reaction,

$$3Fe + {}^3/_4O_2 + 2A_2SO_4 + 3H_3O^+ + {}^3/_2H_2O \rightarrow AFe_3(OH)_6(SO_4)_2 + 3A^+ + 3H_2 \quad (9)$$

As can be seen, H_3O^+ ions are not produced in eq 9; they are consumed. There is no buildup of H_3O^+, thus avoiding the complication of introducing H_3O^+ into the lattice. Indeed, these redox hydrothermal methods have been shown to yield highly pure and highly crystalline jarosites on which reliable magnetic measurements can be acquired,[17,29] as well as large single crystals that have enabled advanced single-crystal neutron studies.[4,5]

The lack of LRO in hydronium jarosite has been attributed to several possibilities,[34] the most recent identifying a "glass-like magnetic state" arising from single-ion anisotropy of the Fe^{3+} ion.[53] This assignment relies on the variations of T_g values in 11 hydronium jarosite samples with varying Fe−O bond lengths. The synthesis of the different hydronium jarosite samples employed in this study relied on the use of methanol under hydrothermal conditions. Fe^{3+} ions are competent oxidants of alcohols, even under conditions much milder than hydrothermal conditions.[54] The oxidation of alcohols by Fe^{3+} ions entails the reduction of the Fe^{3+} ions to Fe^{2+}, which can be incorporated into a jarosite-like lattice.[55] If this is true, inadvertently introduced Fe^{2+} ions in the various hydronium jarosite samples could in principle result in the observed bond-length variations and that they would also likely impact the T_g values. As is the usual case for jarosites, sample impurities, inadvertent chemical defects, and unaccounted-for chemical interactions may play a more important role in physical properties of materials than is often recognized.

Conclusions

A series of potassium-hydronium jarosite solid solutions with systematically varying K^+/H_3O^+ ratios have been prepared by a homogeneous, single-step precipitation procedure. IR spectroscopy shows that proton transfer between the reactive interlayer H_3O^+ ion and the bridging OH^- group of neighboring Fe^{3+} ions is significant. Protonation of the OH^- group leads to an attenuation in the nearest neighboring coupling, though not as much as observed in diiron complexes. For the latter, significant bond length changes attenuate the coupling; in jarosites, the rigidity of the lattice restricts the Fe−O bond distance and changes in distance are small upon protonation. Because the protonation occurs in a chemically disordered way, magnetic disorder is observed in the K^+/H_3O^+ jarosites. This disorder is manifested most prominently in the long-range order of the system. Néel temperatures T_{max} of these antiferromagnets vary considerably, depending on the K^+/H_3O^+ ratio. The T_{max}'s increased with an increasing K^+ content and a decreasing H_3O^+ content between 15.7 and 65.4 K. In some samples, two T_{max} maxima are observed, which indicates the formation of H_3O^+-rich (low T_{max}) and K^+-rich jarosite (high T_{max}) islands. Such islands most likely emerge as a consequence of increasing acidity and a simultaneous depletion of the K^+ ions during the course of the single-step precipitation reaction of jarosites.

Acknowledgment. The authors thank Dr. F. C. Chou for technical assistance in performing magnetic susceptibility measurements and Dr. D. Papoutsakis for helpful discussions. Financial support for this work was provided by the MIT Center for Materials Science and Engineering Research, a MRSEC Program of the National Science Foundation (DMR-9808941).

CM062793F

(51) Maegawa, S.; Nishiyama, M.; Tanaka, N.; Oyamada, A.; Takano, M. *J. Phys. Soc. Jpn.* **1996**, *65*, 2776−2778.
(52) Oakley, G. S.; Visser, D.; Frunzke, J.; Andersen, K. H.; Wills, A. S.; Harrison, A. *Physica B* **1999**, *257*−*268*, 142−144.
(53) Bisson, W.; Wills, A. S. cond-mat/0608234.
(54) Barton, D. H. R.; Beviere, S. D.; Chabot, B. M.; Chavarisi, W.; Taylor, D. K. *Tetrahedron Lett.* **1994**, *35*, 4681−4684.
(55) Rao, C. N. R.; Sampathkumaran, E. V.; Nagarajan, R.; Paul, G.; Behera, J. N.; Choudhury, A. *Chem. Mater.* **2004**, *16*, 1441−1446.